JOURNAL OF APPLIED ELECTROCHEMISTRY 15 (1985) 675–683

Electrochemical behaviour of pure iron in concentrated sodium hydroxide solutions at different temperatures: a triangular potential sweep voltammetric study

V. S. MURALIDHARAN, M. VEERASHANMUGAMANI

Central Electrochemical Research Institute, Karaikudi 623 006, India

Received 11 September 1984

The passivation and dissolution of pure iron in NaOH solutions (1 M–10 M) have been studied at 30°, 60° and 80° C by triangular potential sweep voltammetry. The variation of peak height and peak potential with sweep rates for the three anodic peaks in the forward direction and two cathodic peaks in the backward direction when polarized from − 1.30 V in 1.0 M NaOH solution, suggest that a monolayer adsorption model holds good. The appearance of limiting currents at higher concentrations of NaOH has been explained in terms of the chemical dissolution of two oxides formed by successive oxidation. The formation of different oxides, hydroxides and solution soluble species under transient conditions has been discussed.

1. Introduction

The electrochemical behaviour of the iron–concentrated alkali interface is of basic and practical interest. The corrosion of cast iron and steel nozzles in water electrolysis plant using concentrated alkali and the discharge characteristics of iron electrodes in alkaline batteries necessitate the need to understand the behaviour of oxides, the direct dissolution of the metal and the reductive dissolution of the oxides.

The study of anodic behaviour in 10 M solutions [1] at 80° C suggested that the passive layer is Fe_3O_4. At −0.91 V vs SHE the reduction of magnetite is said to take place [2]. X-ray data and experiments carried out revealed the presence of Fe_3O_4. In the discharge of iron electrodes [3–5] in alkaline solutions, typically 5 M KOH, most of the metal is oxidized to $Fe(OH)_2$ at the first discharge plateau, and the second plateau is due to the mixture of FeOOH and Fe_3O_4. Scanning electron microscope studies [6] revealed the formation of $Fe(OH)_2$ during the first discharge; on continuous discharge the product on the electrode became a sludge, probably of FeOOH. Mossbauer spectroscopy [7, 8] identified the phases *in situ* during the cyclic galvanostatic oxidation–reduction of iron. The first anodic arrest is due to $Fe(OH)_2$ and the second due to β-FeOOH and unreacted $Fe(OH)_2$. On numerous occasions it has been pointed out that the formation of oxides involves soluble Fe (II) and Fe (III) species [9, 10]. Using a gold ring and iron disc system at higher temperatures and in concentrated solutions, Fe (II) soluble species have been detected [11, 12]. The dissolution of higher valence oxides giving rise to soluble Fe (III) species has also been suggested [13].

Single and repetitive cycle voltammetry has been studied earlier [14–17] in alkali solutions at room temperatures and above. The distortion of *E–i* curves at higher concentrations and higher temperatures form the basis of this work.

2. Experimental details

The electrodes were prepared from Swedish iron sheets (99.95% Fe, 0.025% C, 0.0056% Mn, 0.011% S) and made into discs of 0.5 cm^2 area. The discs were embedded in Teflon gaskets with provision for electrical connections. The specimens were polished with 1/0, 2/0, 3/0 and 4/0 emery papers successively. The solutions were deoxygenated by bubbling purified hydrogen for

0021-891X/85 $03.00 + .12

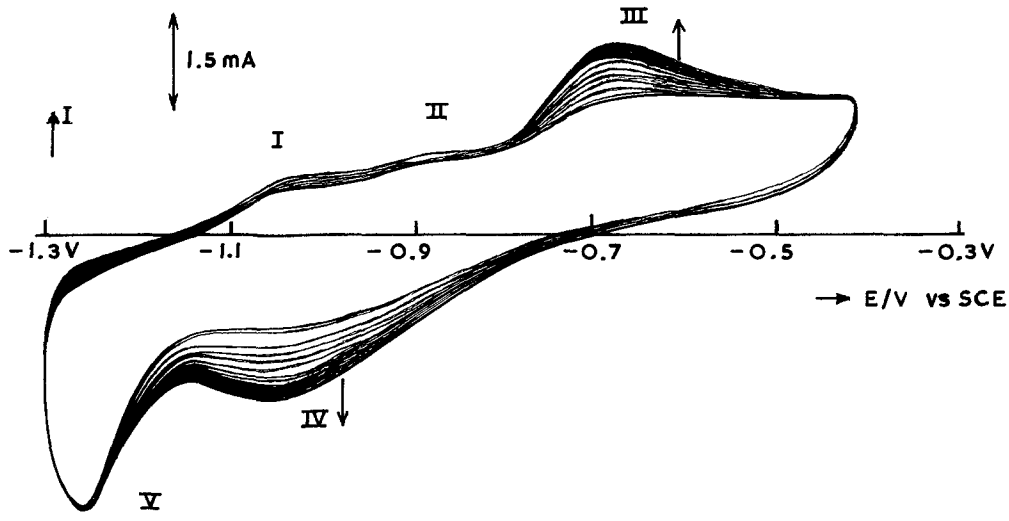

Fig. 1. Typical cyclic voltammogram for pure iron in 1.0 M deoxygenated NaOH solution at 30° C. Sweep rate = 200 mV s^{-1}. $E\lambda_a$ = −0.450 V.

1 h. The experimental set up, comprising a solid state low frequency function generator, potentiostat, *x–y–t* recorder and digital multimeter has been described in detail in an earlier publication [18]. Experiments in duplicate were carried out at 30°, 60° and 80° ± 0.01° C. Potentials were measured against SCE and no corrections were made for liquid junction potentials.

3. Results

The electrode was kept at −1.30 V for 5 min, disconnected, shaken free of adsorbed hydrogen bubbles and polarized to different values. This potential was fixed after several experiments to get reproducible *E–i* curves for different sweep rates (20–600 mV s^{-1}) from −1.3 V to 0.8 V where oxygen evolution takes place. In all concentrations and temperatures the shape of the *E–i* curve is not affected after −0.4 V if the anodic terminating potential ($E_{\lambda,a}$) is changed from −0.4 V and all potentials noble to that.

3.1. *Behaviour in 1.0 MNaOH solutions*

At 30° C and at higher sweep rates (Fig. 1) the voltammogram presents an electrochemical spectrum which has three peaks in the forward and two peaks on the reverse scan. The anodic peaks appear at −1015 mV (I), −890 mV (II) and −685 mV (III) and the cathodic peaks at −1050 mV (IV) and −1250 mV (V). Below 160 mV s^{-1} the anodic peaks I and II disappear and peak III becomes predominant, while there is no change in the backward scan. On repetitive scanning at higher sweep rates the current flowing under peaks III and IV increases with increase in scan number suggesting that they are conjugated, while the charge at peak V seems to be independent. If the forward scan is terminated at −800 mV (positive to equilibrium potential, E_e, of Fe–$Fe(OH)_2$) there is no peak at −1050 mV on the reverse scan while at −1250 mV a distinct peak appears.

At 60° C and 80° C the forward scan at 600 mV s^{-1} reveals three anodic peaks at −1050 mV, −850 mV and −710 mV while the reverse scan reveals cathodic peaks at −1055 and −1245 mV. With increase in scan number (repetitive cycling), the charge flowing under peaks I, II and V remains constant while that of III and IV increases continuously. The measurement of the first anodic peak current was carried out by measuring from the residual current to the peak of the anodic wave. The second and third anodic peak currents were measured from the foot of the respective waves. The cathodic peak currents were measured during the reverse scan from the foot of the respective waves. The dependence of peak current (i_p) and peak potential (E_p) on sweep rates (v) were studied. The currents observed on cyclic sweeping are of the

Table 1. Mechanistic parameters derived from polarization curves for 1.0 M NaOH solution

Peaks	$(\partial E_p/\partial \log v)_{OH^-}$ (*mV per decade*)			$(\partial \log i_p/\partial \log v)_{OH^-}$		
	30° C	*60° C*	*80° C*	*30° C*	*60° C*	*80° C*
I	–	38 ± 5	–	–	0.9 ± 0.1	–
II	–	36 ± 5	–	–	1.0 ± 0.1	–
III	44 ± 5	50 ± 5	45 ± 5	0.76 ± 0.1	1.0 ± 0.1	1.0 ± 0.1
IV	38 ± 5	30 ± 5	48 ± 5	0.7 ± 0.1	0.8 ± 0.1	0.89 ± 0.1
V	25 ± 5	35 ± 5	53 ± 5	1.0 ± 0.1	0.5 ± 0.1	0.51 ± 0.1

order of $10\,mA\,cm^{-2}$ while the double layer charging current, assuming a capacitance of $100\,\mu F\,cm^{-2}$ over the entire potential range is $30\,\mu A\,cm^{-2}$. Hence, the observed currents are principally due to a pseudo capacitative oxide formation–reduction phenomenon. If passivation is of the phase type, the dependence of peak potential and peak current on the square root of sweep rate must be linear. In all cases E_p vs $\log v$ and $\log i_p$ vs $\log v$ give linear plots. This suggests that the discharge of hydrogen ions onto the metal is irreversible and that the electrochemical adsorption model is applicable [19]. Then

$$E_p = \left(\frac{2.3\,RT}{\alpha F}\right) \log v \qquad (1)$$

and

$$Q = \left(\frac{2.718\,RT}{\alpha F v}\right) i_p \qquad (2)$$

for a particular sweep rate. The parameters obtained in 1.0 M NaOH solutions at different temperatures are given in Table 1.

3.2. *Behaviour in 6.0 M NaOH solution*

At 30° C the *E–i* curves reveal a broad anodic peak at −975 mV and a small peak at −700 mV in the forward scan, and a single cathodic peak at −1050 V in the reverse scan. Increase of scan number increases the charge under peak I (−975 mV) while for peak II (−700 mV) and III (−1050 mV) it decreases. The second peak disappears with sweep rates higher than $85\,mV\,s^{-1}$ (Fig. 2). At 60° C two small peaks appear at

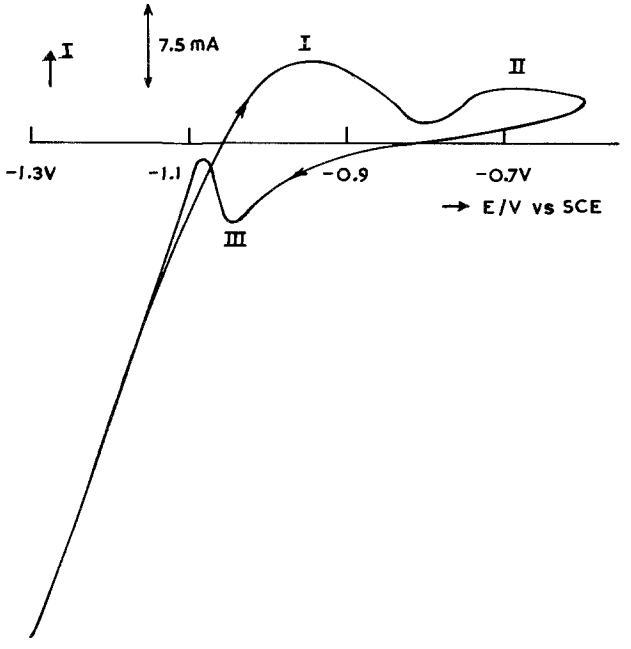

Fig. 2. Typical cyclic voltammogram for pure iron in 6.0 M deoxygenated NaOH solution at 30° C. Sweep rate = $85\,mV\,s^{-1}$. $E\lambda_a = -0.6$ V.

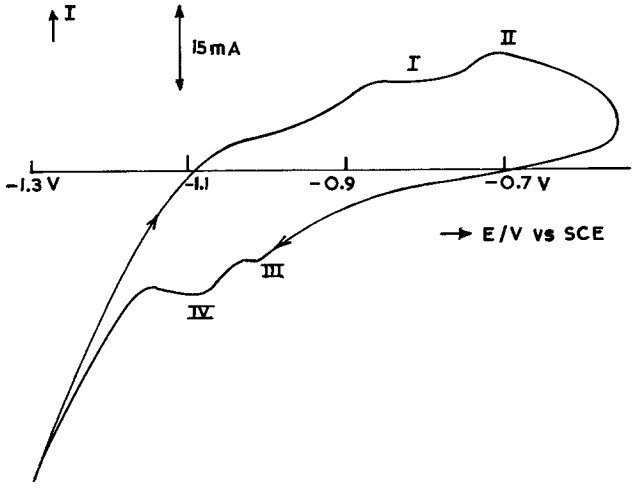

Fig. 3. Typical cyclic voltammogram for pure iron in 6.0 M deoxygenated NaOH solution at 60° C. Sweep rate = 400 mV s^{-1}. $E\lambda_a = -0.5$ V.

60 mV s^{-1} in the forward scan and a single cathodic peak (−1100 mV) on the reverse scan. On increasing the sweep rate above 60 mV s^{-1} a plateau I (−900 mV) and a broad peak II at −725 mV appears in the forward scan, and a shoulder III at −1025 mV and a sharp peak IV at −1075 mV appears in the reverse scan (Fig. 3).

At 80° C a sharp anodic peak I at −890 mV (independent of sweep rate) appears in the forward scan and a cathodic peak II at −1070 mV appears in the reverse scan (Fig. 4). On repeated cycling the charge flowing under these peaks increases, suggesting that the reactions are conjugated.

3.3. *Behaviour in 10 M NaOH solution*

An anodic peak I at −975 mV (sweep rate dependent) and a plateau II around −700 mV in the forward scan, and a sharp cathodic peak III at −1070 mV on the reverse scan appear at 30° C at sweep rates below 160 mV s^{-1} (Fig. 5). On repeated cycling the first peak flattens while the second plateau becomes sharp; the charge consumed at the second peak increases. At sweep rates above 160 mV s^{-1} the single well-defined anodic peak obtained at −900 mV is independent of sweep rate and the current falls to a minimum afterwards.

Studies carried out at 60° C and 80° C (Fig. 6) reveal a single well-defined anodic peak I around −875 mV and the reverse scan reveals a cathodic peak II at −1050 mV. The plots of E_p and $\log i_p$ with $\log v$ were linear. On repeated cycling the anodic peak potential remains constant while the cathodic peak potentials shift towards more active values. This suggests that the overpotential for the reduction reaction is

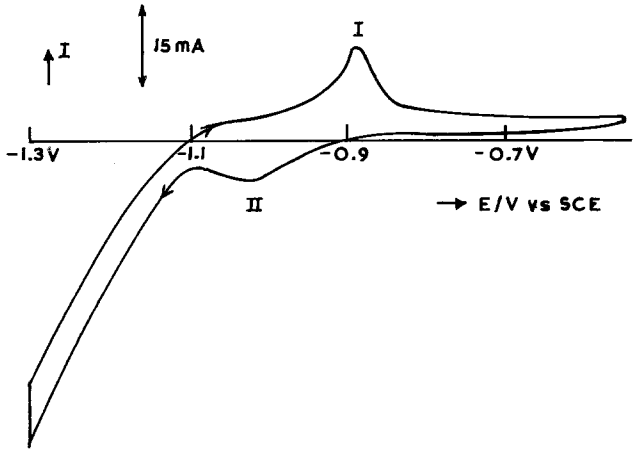

Fig. 4. Typical cyclic voltammogram for pure iron in 6.0 M deoxygenated NaOH solution at 80° C. Sweep rate = 100 mV s^{-1}. $E\lambda_a = -0.5$ V.

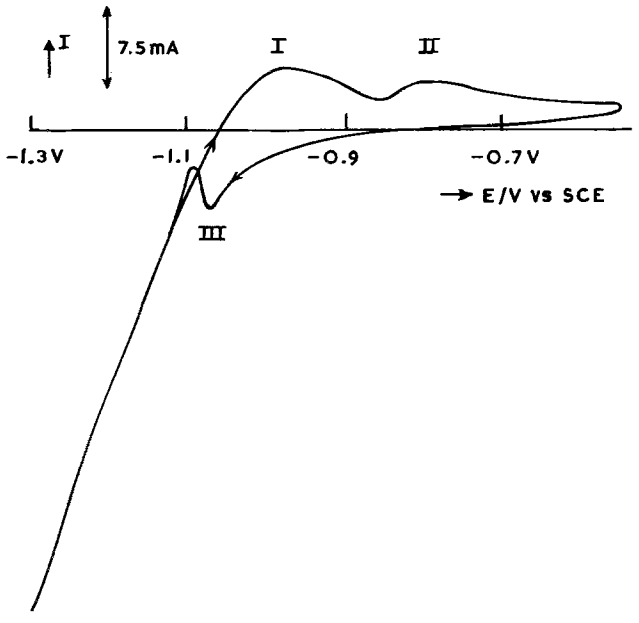

Fig. 5. Typical cyclic voltammogram for pure iron in 10.0 M deoxygenated NaOH solution at 30° C. Sweep rate = 60 mV s^{-1}. $E\lambda_a = -0.55$ V.

enhanced due to non-availability of the species formed in the forward scan. The charge consumed under both the peaks increases on repeated cycling, suggesting that they are conjugated.

4. Discussion

X-ray, electron diffraction and electrochemical methods have identified the anodic films formed as Fe $(OH)_2$, Fe_3O_4, Fe_2O_3 and γ-$Fe_2O_3 \cdot H_2O$ under varying conditions. Comparing cyclic voltammetric peak potentials with thermodynamic potentials, though dangerous, is useful in checking the proposed oxidation–reduction mechanism in the light of the equilibrium potentials of varying reactions. The oxidation–reduction processes may involve overpotentials, and a necessary condition for an oxidation

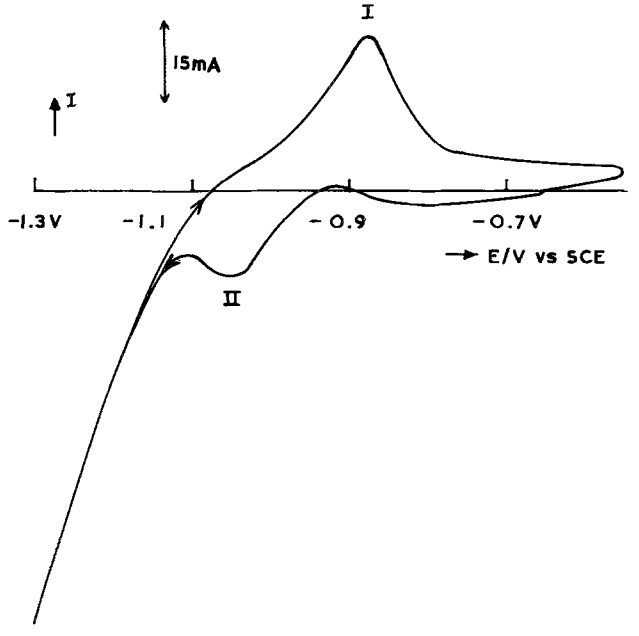

Fig. 6. Typical cyclic voltammogram for pure iron in 10.0 M deoxygenated NaOH solution at 60° C. Sweep rate = 200 mV s^{-1}. $E\lambda_a = -0.55$ V.

process to take place is $E_p > E_e$ or E_p should occur at potentials noble to E_e. Similarly, a reduction process can occur at potentials negative to E_e (i.e. $E_p < E_e$). Equilibrium potentials have been calculated (Table 2) using the Atlas of Electrochemical Equilibria [20].

In 1.0 M solution the current peaks I, II and V are closely related and the peaks III and IV are conjugated. Peak I is due to the electro-oxidation of adsorbed hydrogen on the electrode in the initial stages of oxidation; peak II is due to the conversion of Fe to $Fe(OH)_2$ as it appears at potentials noble to E_e of Fe–$Fe(OH)_2$; peak V is due to the reduction of $Fe(OH)_2$ to Fe. Peak III may be due to the oxidation of $Fe(OH)_2$ to FeOOH.

Since

$$Fe + 2H_2O \rightleftharpoons Fe(OH)_2 + 2H^+ + 2e \quad (3)$$

$$E_e = -0.047 - 0.0591\ pH \text{ at } 25^\circ C$$

$$Fe(OH)_2 \rightleftharpoons [FeOOH] + H^+ + e \quad (4)$$

$$E_e = 0.271 - 0.0591\ pH \text{ at } 25^\circ C$$

$$3Fe(OH)_2 \rightleftharpoons Fe_3O_4 + 2H_2O + 2H^+ + 2e \quad (5)$$

$$E_e = -0.202 + 0.0591\ pH \text{ at } 25^\circ C$$

the potential difference is 318 mV for FeOOH and -155 mV for Fe_3O_4 at constant pH and temperature. The observed potential difference at 205 mV is due to the change in OH^- ion activity at the electrode caused by potential sweeping. Hence it is due to the conversion of $Fe(OH)_2$ to FeOOH. The peak IV is due to the reduction of FeOOH to $Fe(OH)_2$ which subsequently undergoes reduction to Fe. This is similar to those results reported earlier [15].

On repeated cycling at higher temperatures the charge flowing under peaks I, II and V remains constant while under peaks III and IV it increases continuously, suggesting the direct conversion of Fe to FeOOH in parallel to the formation of $Fe(OH)_2$. On reverse scan the [FeOOH] formed undergoes reductive dissolution to $HFeO_2^-$. The charge flowing under peaks III and IV increases with repeated cycling suggesting that more and more [FeOOH] dissolves to form $HFeO_2^-$ and not $Fe(OH)_2$. If more and more $Fe(OH)_2$ had been formed on repetitive cycling then the charges under peak V would have increased. Direct reduction of [FeOOH] to Fe is not favoured at the potential in which the peak appears.

In 6 M NaOH solutions at 30° C the occurrence of peaks at -975 and -700 mV is due to the formation of $Fe(OH)_2$ and FeOOH respectively, and the cathodic peak is due to the reduction of $Fe(OH)_3$–FeOOH to $Fe(OH)_2$ which can dissolve in higher alkali concentration giving $HFeO_2^-$. Since all the $Fe(OH)_2$ that was formed dissolved to yield soluble Fe(II) species, there is no peak corresponding to the reduction of $Fe(OH)_2$ to Fe.

The results obtained at 60° C are interesting. The appearance of a plateau at sweep rates above 60 mV s^{-1} is due to the chemical dissolution of the oxides formed or to thickening of the oxide film. The charge under the anodic plateau (Q_a) is always greater than that for the cathodic peak (Q_c) at all sweep rates, suggesting that chemical dissolution of oxide can take place at elevated temperatures.

From the theory of electrochemical formation of metallic oxides using a chrono-amperometric method with linear variation of potential [21] the appearance of a limiting current of plateau in the E–i curves indicates cases where one or both oxides are soluble with the formation of oxide or oxides obeying Langmuir and Temkin–Frunkin conditions.

In 1.0 M NaOH solution the linear plots of E_p vs log v and log i_p vs log v for the anodic peaks suggest formation of $Fe(OH)_2$ and [FeOOH] monolayers or a layer of constant thickness. The slope of the $E_{p,II}$ vs log v plot for the first potential sweep is $\simeq 40$ mV per decade; this may indicate the formation of a $Fe(OH)_2$ film with a low degree of coverage obeying the Langmuir adsorption isotherm. The $E_{p,III}$ vs log v plot for the third peak reveals a Tafel slope of 40 ± 5 mV; this suggests the following reaction sequence:

$$Fe + OH^- \rightleftharpoons [Fe(OH)]_{ad} + e \quad (6)$$

$$[Fe(OH)]_{ad} \longrightarrow [Fe(OH)]_{ad}^+ + e \quad (7)$$

$$[Fe(OH)]_{ad}^+ + OH^- \rightleftharpoons Fe(OH)_2 \quad (8)$$

$$Fe(OH)_2 + OH^- \rightleftharpoons [FeOOH] + H_2O + e \quad (9)$$

Table 2. Possible oxidation–reduction schemes and associated equilibrium potentials (mV vs SCE)

Reactions	*pH = 13*			*pH = 14*			*pH = 15*		
	30° C	*60° C*	*80° C*	*30° C*	*60° C*	*80° C*	*30° C*	*60° C*	*80° C*
$3HFeO_2^- + H^+ \rightleftharpoons Fe_3O_4 + 2H_2O + 2e$	−1683	−1670	−1611	−1653	−1637	−1576	−1624	−1604	−1541
$3Fe(OH)_2 + H_2O \rightleftharpoons Fe_3O_4 + 2H^+ + 2e$	−1209	−1300	−1352	−1268	−1366	−1422	−1327	−1423	−1492
$3Fe + 4H_2O \rightleftharpoons Fe_3O_4 + 8H^+ + 8e$	−1092	−1183	−1235	−1151	−1249	−1305	−1210	−1315	−1375
$Fe + 2H_2O \rightleftharpoons Fe(OH)_2 + 2H^+ + 2e$	−1052	−1143	−1195	−1111	−1209	−1265	−1170	−1275	−1335
$Fe + 3H_2O \rightleftharpoons Fe(OH)_3 + 2H^+ + 2e$	−978	−1069	−1121	−1037	−1135	−1191	−1096	−1201	−1261
$Fe + 2H_2O \rightleftharpoons HFeO_2^- + 3H^+ + 2e$	−914	−1031	−1109	−1004	−1130	−1214	−1094	−1229	−1319
$Fe(OH)_2 + H_2O \rightleftharpoons Fe(OH)_3 + H^+ + e$	−1050	−1141	−1193	−1109	−1207	−1263	−1168	−1273	−1333

In 6.0 M NaOH solutions at 30° C, the $E_{p,II}$ vs log v linear plot gives a slope of 110 ± 15 mV and $(\delta \log i_p/\delta \log v)_{OH^-} = 0.9 \pm 0.1$, suggesting that Reaction 9 with equilibrium potential $E_e = 0.271 - 0.0591$ pH at 25° C involves charge transfer as the rate determining step (rds).

In 6.0 M NaOH solution at 60° C, the formation of $Fe(OH)_2$ involves Reaction 7 as the formation of [FeOOH] involves Reaction 9 as the rds. The appearance of limiting currents near the formation of these two oxides indicates a potential independent process. These oxides can dissolve chemically to yield soluble Fe (II) and Fe (III) species.

At 80° C in 6.0 M NaOH solution the appearance of a single anodic peak is due to the dissolution of iron via $Fe(OH)_2$ formation. The $Fe(OH)_2$ formed initially undergoes chemical dissolution to give $HFeO_2^-$:

$$Fe(OH)_2 + OH^- \rightleftharpoons H\,FeO_2^- + H_2O \quad (10)$$

The soluble $HFeO_2^-$ formed undergoes further oxidation at high anodic potentials to give FeO_2^-, a soluble Fe (III) species. These two soluble species can combine to form Fe_3O_4:

$$HFeO_2^- \rightleftharpoons FeO_2^- + H^+ + e \quad (11)$$

$$HFeO_2^- + 2FeO_2^- + H_2O \rightleftharpoons Fe_3O_4 + 3\,OH^- \quad (12)$$

In 10.0 M NaOH solutions the appearance of an anodic peak I and a limiting current around −800 mV suggest that both oxides are soluble and yield Fe (II) and Fe (III) species, and that the reduction reaction is the conversion of [FeOOH] to $Fe(OH)_2$ or $HFeO_2^-$. At faster sweep rates the direct oxidation of iron to $HFeO_2^-$, FeOOH or Fe (III) soluble species via $Fe(OH)_2$ as intermediate occurs and the cathodic reaction is the reduction of FeOOH to $Fe(OH)_2$ which chemically dissolves to yield $HFeO_2^-$.

The overall electrochemical behaviour involved in the passivation and dissolution of iron in NaOH solutions should involve hydroxo, oxy species along with soluble $HFeO_2^-$, FeO_2^{2-} or Fe (III) species under non-steady-state conditions.

$$Fe + OH^- \rightleftharpoons [Fe(OH)]_{ad} + e \quad (13)$$

$$[Fe(OH)]_{ad} \longrightarrow [Fe(OH)^+]_{ad} + e \quad (14)$$

$$[Fe(OH)^+]_{ad} + OH^- \rightleftharpoons Fe(OH)_2 \quad (15)$$

These steps are the same as proposed for iron dissolution in acid media [15]. The transformation of $[Fe(OH)^+]_{ad}$ to soluble Fe (II) species or $Fe(OH)_2$ depends on pH and temperature.

In 6 M NaOH solutions and temperatures above 60° C $[Fe(OH)^+]_{ad}$ can transform into $HFeO_2^-$ as

$$[Fe(OH)^+]_{ad} + 2OH^- \longrightarrow H\,FeO_2^- + H_2O \quad (16)$$

At higher anodic potentials $Fe(OH)_2$ can react with OH^- to form FeOOH as

$$Fe(OH)_2 + OH^- \longrightarrow [FeOOH] + H_2O + e \quad (17)$$

The direct oxidation of Fe to FeOOH may also follow the same sequence. [FeOOH] can dissolve to yield Fe (III) species, or $HFeO_2^-$ formed in the solution can undergo oxidation.

$$HFeO_2^- \rightleftharpoons FeO_2^- + H^+ + e \quad (18)$$

or

$$FeOOH + OH^- \rightleftharpoons FeO_2^- + H_2O \quad (19)$$

The species ($HFeO_2^-$) and (FeO_2^-) can form Fe_3O_4

$$HFeO_2^- + 2FeO_2^- + H_2O \longrightarrow Fe_3O_4 + 3OH^- \quad (20)$$

or

$$2[FeOOH] \longrightarrow [Fe_2O_3 \cdot H_2O] \quad (21)$$

The formation of $Fe_2O_3 \cdot H_2O$ involves the formation of FeOOH which is formed by Reactions 13–15 and 17. The formation of Fe_3O_4 is due to the transformation of β-FeOOH via FeO_2^-, a soluble Fe (III) species.

Acknowledgement

The authors wish to thank Professor K. I. Vasu, Director, Central Electrochemical Research Institute, Karaikudi for his interest in this work and for permission to publish this paper.

References

[1] V. V. Losev and B. N. Kabanov, *Zh. Fiz. Khim.* **28** (1954) 824.

[2] A. M. Surkhotin and K. M. Kartashov, *Corros. Sci.* **5** (1965) 393.

[3] T. K. Teplinskaya, N. N. Fedorova and S. A. Rozentsveig, *Zh. Fiz. Khim.* **38** (1964) 2176.
[4] A. J. Salkind, C. J. Venuto and S. U. Falk, *J. Electrochem. Soc.* **111** (1964) 493.
[5] H. G. Silver and E. Leaks, *ibid.* **117** (1970) 5.
[6] L. Ojefers, *ibid.* **123** (1976) 1691.
[7] A. M. Pritchard and B. J. Mould, *Corros. Sci.* **11** (1971) 1.
[8] Y. Geronov, I. Tomov and S. Georgiev, *J. Appl. Electrochem.* **5** (1975) 351.
[9] J. Labat, J. C. Jarrousseatu and J. F. Laurent, Proceedings of Power Sources Conference, Brighton, 1970 (edited by D. H. Collins), ORIEL Press (1971) pp. 283.
[10] T. Hurlen, *Electrochim. Acta* **8** (1963) 609.
[11] R. D. Armstrong and I. Baurhoo, *J. Electro. anal. Chem.* **34** (1972) 41.
[12] R. D. Armstrong and I. Baurhoo, *ibid.* **40** (1972) 325.
[13] D. S. Poa, J. F. Miller and N. P. Yao, Extended Abstracts, Vol. 83-2, Fall Meeting of Electrochemical Society, Washington, DC, October 9–14, 1983, p. 17.
[14] D. D. Macdonald and D. Owen, *J. Electrochem. Soc.* **120** (1973) 317.
[15] D. Geana, A. A. El Miligy and W. J. Lorenz, *J. Appl. Electrochem.* **4** (1974) 337.
[16] R. S. Schrebler Guzman, J. R. Vilche and A. J. Arvia, *Electrochim. Acta* **24** (1979) 395.
[17] D. D. Macdonald and B. Roberts, *ibid.* **23** (1978) 781.
[18] V. S. Muralidharan, K. Thangavel and K. S. Rajagopalan, *ibid.* **28** (1983) 1611.
[19 S. Srinivasan and E. Gileadi, *ibid.* **11** (1966) 321.
[20] M. Pourbaix, 'Atlas of Electrochemical Equilibria in Aqueous Solutions', Pergamon Press, (1966).
[21] A. M. Baticle, R. P. Veerereau and J. Vernieres, *J. Electroanal. Chem.* **45** (1973) 439.